DESIGN AND OPTIMIZATION OF A SEEDBED PREPARATION DEVICE FOR RAPESEED BLANKET SEEDLING TRANSPLANTING IN RICE STUBBLE FIELDS
/
稻茬田油菜毯状苗移栽用苗床整地装置的设计与优化

Qing TANG[1,2,3], Yaodong WU[2], Lan JIANG[1,3], Jixuan WANG[1], Meng BAI[1], Jun WU[1,3], Hongmei JI[2], Qun LI[2]

[1]Nanjing Institute of Agricultural Mechanization, Ministry of Agriculture and Rural Affairs, Nanjing 210014, China;
[2] Jiangsu Yunma Agricultural Machinery Manufacturing Co., Ltd., Yancheng 224100, China
[3] Key Laboratory of Modern Agricultural Equipment, Ministry of Agriculture and Rural Affairs, Nanjing 210014, China

Corresponding author: Jun WU
Tel: +86.15366092905; E-mail: wujun01@caas.cn
DOI: https://doi.org/10.35633/inmateh-78-72

***Keywords**: Rapeseed, Transplanting, Seedbed preparation, Reverse rotary tillage, Straw incorporation, Surface flatness, Seedbed quality, Agricultural machinery optimization*

ABSTRACT

In rice stubble fields with heavy clay soil and full straw retention, conventional tillage practices often fail to create suitable seedbed conditions for rapeseed blanket seedling transplanting. To address this limitation, a novel integrated seedbed preparation device was developed, incorporating reverse rotary tillage for straw crushing and soil fragmentation, midline ditch clearing with lateral soil displacement, and bed leveling combined with slit cutting. Key components, including the reverse rotary blade arrangement, ditch-cleaning shovel, and leveling–slitting roller, were theoretically designed and parametrically optimized. Taking grid bar spacing and soil-retaining soft curtain distance as experimental factors, and the soil fragmentation rate of the topsoil layer as the evaluation index, a full-factorial experiment was conducted. The optimal structural parameters were determined as a grid bar spacing of 75 mm and a soft curtain distance of 500 mm. Based on response surface methodology, field experiments were carried out using forward speed, rotary shaft speed, and leveling roller speed as factors, and soil fragmentation rate, straw incorporation rate, and surface flatness as evaluation indicators. The optimal operating parameters were identified as a forward speed of 0.8 m/s, a rotary blade speed of 243 r/min, and a leveling roller speed of 180 r/min. Under these conditions, the soil fragmentation rate reached 98.92%, the straw incorporation rate was 87.81%, and the surface flatness was 15.14 mm. The proposed device significantly improves seedbed quality in cohesive, straw-rich paddy fields, providing a reliable technical solution for the mechanized transplanting of rapeseed blanket seedlings.

摘要

在粘重土壤和全秸秆还田的稻茬地，传统耕作方法难以为油菜毯状苗移栽创造合适的苗床。针对这一问题，开发了一种新型苗床整地装置，采用反旋碎秸，中间开沟、平畦切缝平整苗床。对关键部件，包括反向旋耕刀排列、清沟铲和平土辊进行了理论设计和参数优化。以挡草栅间距和挡土软帘距离为因素，以耕层表层碎土率为指标进行全因素试验，得到最优挡草栅间距为 75mm，挡土软帘距离为 500mm。基于响应曲面法进行田间试验，以评估前进速度、旋耕刀速度和平土辊速度对土壤破碎率、秸秆掩埋率和地表平整度的影响。结果显示最佳参数为:前进速度 0.8 m/s, 旋转刀片速度 243 r/min, 平整辊速度 180 r/min。在此条件下, 碎土率达到 98.92%, 秸秆掩埋率达到 87.81%, 地表平整度达到 15.14 mm。该装置有效地提高了黏重土壤秸秆全量还田的苗床质量, 为油菜毯状苗机械化移栽提供了可靠的技术解决方案。

INTRODUCTION

Rapeseed is one of the major oil crops in China. In the rice-rapeseed rotation areas of the Yangtze River Basin, approximately 40% of rapeseed cannot be directly sown due to the delayed harvest of the preceding rice crop, necessitating seedling raising and transplanting. Seedbed preparation prior to transplanting is a critical process that affects the survival rate of rapeseed seedlings after transplanting and their subsequent growth. Through tillage practices such as soil fragmentation, straw incorporation and seedbed surface leveling, a suitable transplanting condition characterized by loose soil structure and flat surface can be established (*Dai F. et al., 2011*).

However, the rice stubble fields feature high soil moisture content and a large amount of crop residues from full straw incorporation. Traditional tillage methods are prone to problems such as component adhesion, soil compaction, uneven soil fragmentation and poor straw mulching effect, which make it difficult to meet the stringent requirements of seedbed quality for rapeseed blanket seedling transplanting (*Ucgul M. et al., 2014*).

Tillage quality is affected by multiple factors such as soil physical properties, geometric parameters of cutting tools, and motion parameters *(Nidal H.A. et al., 2003*). For seedbed preparation, scholars at home and abroad have carried out a series of studies focusing on tillage methods, machine components, and flatness detection. Early studies focused on the effects of tillage on soil structure, seed-soil contact, and seedling emergence, pointing out that seedbed flatness is one of the key indicators for evaluating seedbed quality, and an uneven seedbed will increase the risk of seedling mortality (*Håkansson et al., 2002; Dürr et al., 2000*). Appropriate soil treatment can improve the physical structure of seed bed and be beneficial to the development of crop roots *(Alagbo O.O.et al., 2024; Ferreira C.J.B.et al., 2023)*.

In terms of tillage methods, different tillage methods affect weed population distribution and soil conditions in seed beds, and then indirectly affect crop emergence and growth *(Chetan F.et al., 2025)*, reverse rotary tillage has shown advantages under the condition of straw returning due to its characteristics such as low resistance, flat bottom of the tillage layer, and good covering performance (*Ding W.M. et al., 2001, 2003; Shibusawa, 1993*). In terms of machinery and equipment, research has involved the arrangement of rotary tillage blades, soil throwing performance, and the design of ditching and leveling components (*Jia H.L. et al., 2000; Liao Y.T. et al., 2020*). In addition, seedbed flatness detection and control technologies based on laser scanning and machine vision have also provided support for precise operations (*Jensen et al., 2017; Riegler et al., 2020*). However, when facing the synergistic effect of heavy clay soil and high straw content in rice stubble fields, existing studies still lack systematic machinery schemes and parameter optimization for achieving integrated operations of efficient soil fragmentation, deep straw burial, synchronous ditching, ridging, and slit cutting.

To address the aforementioned limitations, this study proposes a seedbed preparation device for rapeseed blanket seedling transplanting, suitable for heavy clay soils with full straw incorporation in rice stubble fields. The device integrates multiple operational processes, including *reverse rotary tillage for straw crushing, central splitting with lateral soil displacement, ditching and ridging, layered placement of soil and straw, and seedbed leveling combined with slit cutting*. First, through theoretical analysis, the arrangement of reverse rotary tillage blades, their motion parameters, and the structural and kinematic parameters of key components, such as the ditching shovel and the seedbed leveling-slitting roller, were determined. Second, field experiments were conducted to investigate the effects of key operating parameters (forward speed, rotary blade shaft speed, and leveling roller speed) on soil fragmentation rate, straw incorporation rate, and seedbed surface flatness, and regression models were established for parameter optimization. Finally, validation experiments were performed to evaluate the operational performance of the optimized device, providing both a reliable technical solution and a theoretical basis for high-quality seedbed preparation in mechanized rapeseed transplanting.

MATERIALS AND METHODS

Device description and agronomic requirements

As shown in Fig. 1, the seedbed preparation device mainly consists of a frame, housing, rotary tiller blade group, straw-retaining grid, power transmission assembly, adjustment mechanism, rollers, soil leveling roller, floating device, and other auxiliary components.

The device is mounted on a tractor, which provides the driving power. The rotary tiller blade group operates in reverse rotation, cutting the soil from bottom to top and conveying the mixture of soil, stubble, and straw rearward through the clearance between the upper section and the housing. After impacting the rigid straw-retaining grid, larger soil clods, stubble, and straw lose momentum and fall, while finer soil particles and small straw fragments continue moving backward, subsequently contacting the flexible soil-retaining curtain and sliding downward along its surface. As a result, fine soil covers the underlying stubble, straw, and large soil clods, forming a layered seedbed structure in which coarse materials are distributed in the lower layer and fine soil is concentrated in the upper layer. Finally, the soil leveling roller performs active rolling on the surface layer, simultaneously leveling and compacting the seedbed. At the same time, the slitting discs mounted on the leveling roller create planting slits in the surface soil, while trapezoidal seedbed furrows are formed by the conical discs.

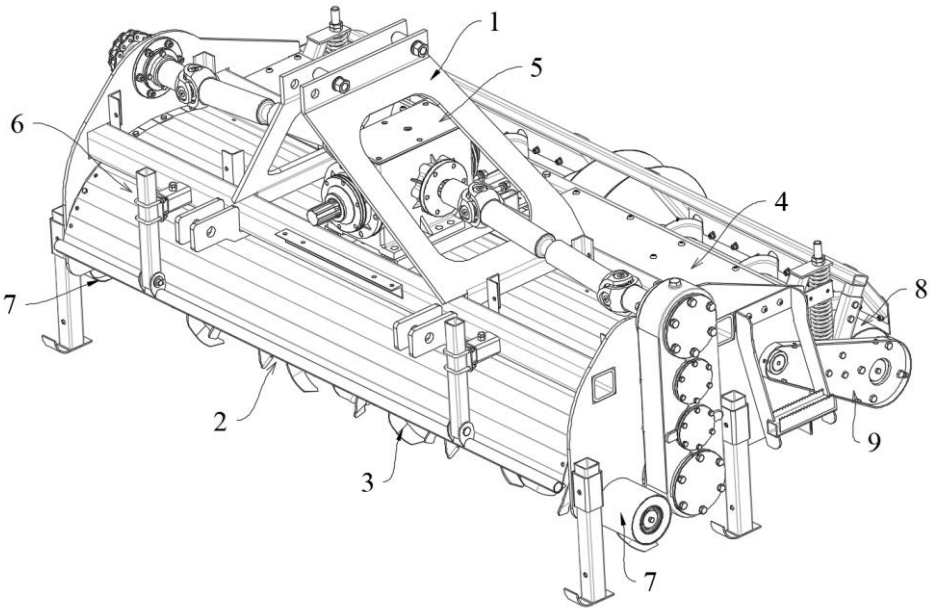

Fig. 1 - Structure diagram of seedling bed preparation device

1.Frame; 2. Housing; 3. Rotary tiller blade group; 4. Straw-retaining grid; 5. Power transmission assembly; 6. Adjustment mechanism; 7. Roller; 8. Soil leveling roller; 9. Floating device

The agronomic requirements for rapeseed cultivation in the Yangtze River Basin of China specify a ridge width of 1.8–2.0 m, a furrow width of 15–20 cm and a furrow depth of 18–20 cm. Meanwhile, it is required to minimize furrow collapse, ensure compaction on both sides of the furrow, and adopt a trapezoidal cross-section for the furrow. As shown in Fig. 2 for the ridge cross-section: L_1 is the ridge top width, measuring 1800 mm; L_2 is the ridge bottom width, measuring 1860 mm; l_1 is the furrow top width, measuring 260 mm; l_2 is the furrow bottom width, measuring 200 mm; H is the furrow depth, measuring 180 mm. Sufficient growth space should be reserved for rapeseed seedlings on both sides of the furrow, so the margin between the seedlings and the furrow edge must meet the relevant requirements. With reference to agronomic standards, the margin ***e*** is set at 150 mm. The planting row spacing ***s*** is determined as 300 mm to match the seedling tray for blanket seedlings. Through comprehensive calculation, the working width L is set at 2300 mm.

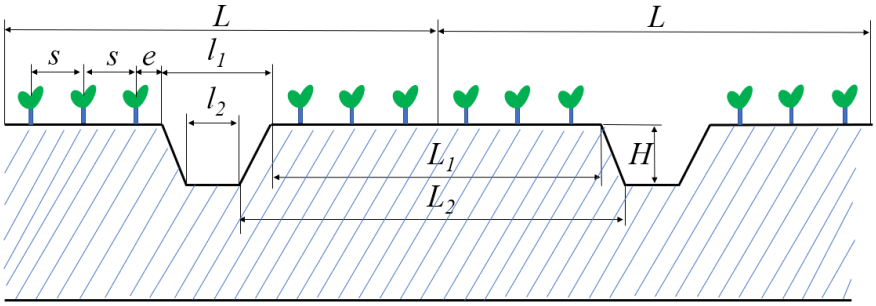

Fig. 2 - Scheme diagram of rapeseed blanket seedling transplanting process

Kinematic analysis of reverse rotary tillage

During operation, the rotary tillage blade rotates around the cutter shaft and moves forward. A Cartesian coordinate system is established with the rotation center of the cutter shaft as the origin, where the forward direction of the rotary tiller is defined as the positive direction of the x-axis, and the vertically upward direction is the positive direction of the y-axis (Fig. 3). Let the forward speed of the unit be V_m and the angular velocity of the cutter shaft be ω; then the motion equation of the rotary tillage blade tip is expressed as follow :

$$\begin{cases} x = R\cos\omega t + v_m t = R(\cos a + a/\lambda) \\ y = R\sin\omega t = R\sin a \end{cases} \quad (1)$$

where:

x, y is position coordinates of the rotary tillage blade tip at any moment; R is rotational radius of the rotary tillage blade tip (swing radius of the cutter roller), [mm]; a is rotation angle of the rotary tillage blade, $a=\omega t$, [°]; λ is rotary tillage speed ratio, $\lambda = R\omega/v_m$; t is time, [s].

Equation (1) describes the absolute motion of the reverse rotary tillage blade tip. Its trajectory exhibits different shapes and characteristics depending on the swing radius R of the cutter roller, the angular velocity ω of the cutter shaft, and the forward speed v_m of the unit. By differentiating Equation (1) with respect to time, the component velocities of the rotary tillage blade tip in the x-axis and y-axis directions can be obtained as follows:

$$\begin{cases} v_x = dx/dt = v_m - R\omega \sin \omega t = v_m(1 - \lambda \sin a) \\ v_y = dy/dt = R\omega \cos \omega t = R\omega \cos a \end{cases} \quad (2)$$

At this point, the magnitude of the absolute velocity v of the rotary tillage blade tip is expressed as follows:

$$v = \sqrt{{v_x}^2 + {v_y}^2} = \sqrt{{v_m}^2 + R^2\omega^2 - 2v_m R\omega \sin \omega t} = v_m\sqrt{\lambda^2 + 1 - 2\lambda \sin a} \quad (3)$$

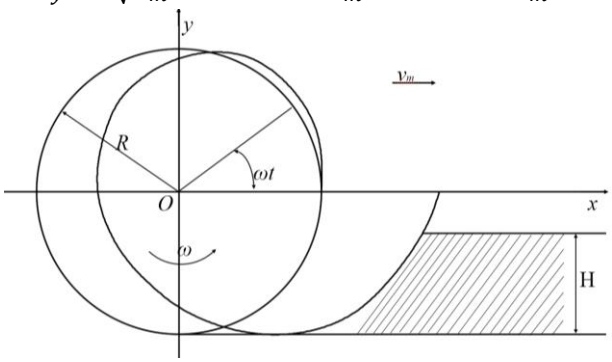

Fig. 3 - Motion trajectory of rotary blade

It can be seen from Equation (2) that within its main soil-cutting range ($3\pi/2 < a < 2\pi$), the horizontal component velocity v_x of the rotary tillage blade tip is in the same direction as the forward speed v_m of the rotary tiller. Therefore, whether $\lambda > 1$ or $\lambda < 1$, the blade maintains its soil-cutting function. Thus, the rotary tillage speed ratio can be appropriately reduced to decrease the rotational speed of the cutter shaft. The soil-cutting position of the reverse rotary tillage blade is located at the part with the minimum curvature of the cycloid. Hence, even when the soil-cutting pitch is relatively large, the height of the bulge at the furrow bottom caused by reverse rotary tillage is relatively small, and the bottom of the tilled layer remains relatively flat after tillage. Studies have shown that reverse rotary tillage is a relatively superior tillage method (*Shibusawa S., 1993*).

The value of the rotary tillage speed ratio λ directly affects the motion trajectory of the rotary tillage blade tip and determines the soil clod cutting performance of the rotary tillage blade. Plots were made for three cases where the rotary tillage speed ratio λ was set at 0.5, 1, and 3, and the motion trajectories of the blade tip under different rotary tillage speed ratios are shown in Fig. 4.

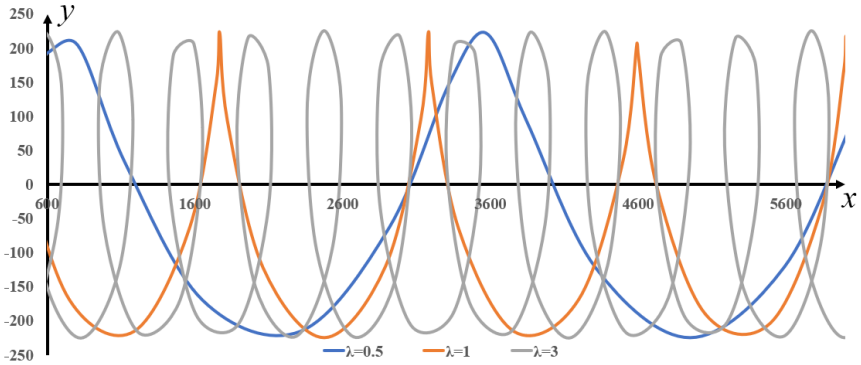

Fig. 4 - Tip trajectory of reverse rotary tillage under different rotary tillage speed ratio

It can be observed from Fig. 4 that as the rotary tillage speed ratio λ increases continuously (as indicated by the definition of λ, this means the rotational speed of the rotary tiller shaft increases when the forward speed remains constant), the rotation frequency of the rotary tillage blade rises accordingly. As a result, the number of soil-cutting operations per unit time increases, generating a stronger cutting impact on the soil and rice stubble, which is conducive to soil cultivation and stubble incorporation (*Peng B., 2014*). Meanwhile, the absolute height of the unevenness at the bottom of the tilled layer after rotary tillage decreases with the increase in λ, that is, the larger the value of λ, the flatter the soil bottom becomes.

Calculation Formula (4) for Rotational Speed of Reverse Rotary Tiller Shaft.

$$n = \frac{60 v_m}{SZ} \tag{4}$$

where: n is rotary tillage speed, [r/min]; v_m is forward speed of the unit, [m/s], adopted as 1 m/s in this study; S is soil-cutting pitch, [m]; Z is number of rotary tillage blades uniformly installed on the same mounting plane of the cutter shaft, adopted as 2 in this study.

Given the heavy clay soil and high straw content in the field, the soil-cutting pitch can be set at 4–6 cm with reference to the *Agricultural Machinery Design Manual* (*Chinese Academy of Agricultural Mechanization Sciences, 2007*). The rotational speed range of existing reverse rotary tillers is 280–348 r/min (*Luo J.M., 2019*). Through comprehensive consideration, the initial rotational speed of the rotary tiller shaft is determined as 310 r/min.

Analysis of soil throwing performance in reverse rotary tillage

The housing surface is curved, but it can be approximated as a plane within a small segment, and thus as a straight line within this plane. As shown in Fig. 5, a static coordinate system xoy is established with the center of the rotary tiller shaft as the origin when the rotary tiller is stationary, the forward direction of the machine as the positive direction of the *x*-axis, and the vertically upward direction as the positive direction of the *y*-axis. A moving coordinate system $x_1o_1y_1$ is established with the endpoint o_1 of the housing as the origin, the direction of the housing as the x_1-axis, and the direction perpendicular to the housing upward as the positive direction of the y_1-axis. In the figure, l denotes the length of the housing, α denotes the angle between the housing and the horizontal direction, l_x denotes the horizontal distance from point o_1 to the center o' of the rotary tiller shaft, and l_y denotes the vertical height between them. Then the motion equations of point $o'(x_{o}', y_{o}')$ and point $o_1(x_{o1}, y_{o1})$ are as follows:

$$\begin{cases} x_o' = v_m t = \frac{R\omega}{\lambda} t \\ y_o' = 0 \end{cases} \tag{5}$$

$$\begin{cases} x_{o1} = x_o' - l_x = \frac{R\omega}{\lambda} t - l_x \\ y_{o1} = l_y \end{cases} \tag{6}$$

Assume that a particle with coordinates (x, y) in the static coordinate system has coordinates (x_1, y_1) in the moving coordinate system. After coordinate transformation, the following relationship is obtained:

$$\begin{bmatrix} x \\ y \end{bmatrix} = \begin{bmatrix} x_{o1} \\ y_{o1} \end{bmatrix} + \begin{bmatrix} cos\alpha & -sin\alpha \\ sin\alpha & cos\alpha \end{bmatrix} \begin{bmatrix} x_1 \\ y_1 \end{bmatrix} \tag{7}$$

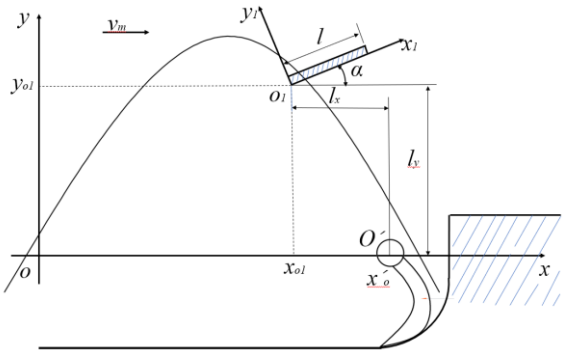

Fig. 5 - Schematic diagram of position relationship between cover and rotary blade

Assuming that a soil clod is cut and thrown, and the throwing point of a soil particle is $P(x_0,y_0)$ with an initial throwing velocity of $v_0(v_{0x}, v_{0y})$, then the motion equation of the soil particle is as follows:

$$\begin{cases} x = x_0 + v_{0x} t \\ y = y_0 + v_{0y} t - \frac{1}{2} g t^2 \end{cases} \tag{8}$$

The height of the upward-moving soil particle must be greater than or equal to the vertical coordinate l_y of the housing. Therefore, the collision conditions for the soil particle are: $x_0+v_{0x}v_{0y}/g \geq x_{01}+v_m v_{0y}/g$ 、 $x_0+v_{0x}v_{0y}/g \leq x_{01}+v_m v_{0y}/g+lsin\alpha$ and $y_0+v_{0y}^2/2g \geq max\ (l_y,\ l_y+l\ sin\alpha)$. Soil particles that collide with the housing will fall onto the rotary tiller blades again and then be thrown backward out of the housing by the high-speed rotating blades.

Design of rotary tiller blade arrangement

The arrangement design shall follow the following principles (*Chinese Academy of Agricultural Mechanization Sciences, 2007*): ①Reduce axial impact load, the rotary tillage curved blades are divided into left-handed and right-handed types, and the left and right curved blades should enter the soil alternately to balance the lateral forces on both sides and reduce the axial impact load on the cutter shaft. ②Stabilize the soil entry frequency of rotary tillage blades: the blades are required to be evenly distributed within one circle of the axial projection of the cutter shaft, which can stabilize the soil cutting resistance and reduce impact. ③ Maximize the circumferential angle between adjacent rotary tillage curved blades and arrange them in a symmetrical spiral pattern to increase the space between the blades and avoid soil clogging (*Li Zixuan et al., 2020; Zhang Chunling et al., 2019*). ④The soil cutting pitch of each blade among the 2 (or more) blades in each soil cutting zone should be as equal or similar as possible to ensure uniform soil fragmentation. ⑤The distance between axially adjacent cutter holders shall be greater than the width of a single blade to reduce missed tillage (*Jia Honglei et al., 2000*).

The double-headed spiral arrangement was selected in accordance with the above principles. Since the ditching scheme was arranged in the middle, it was necessary to minimize the residual soil after rotary tillage in the middle area to reduce ditching pressure. By adjusting the left and right bending directions of the rotary tillage blades within the segment group, soil clods could be thrown to the outer sides of the two segments to form a preliminary ditch, which was then shaped into a formal ditch by the ridger shovel. The tillage width of the rotary tiller was 2300 mm, and the length of the cutter shaft available for installing cutter holders was 2200 mm. The length of the cutter shaft section for installing cutter holders in the middle ditching area was 200 mm, with the thickness of each cutter holder being 22 mm. The distance between the center planes of the cutter holders of two adjacent rotary tillage blades should not be excessively large; conversely, an overly small distance tended to cause soil clogging, especially in rice stubble fields where soil aggregates were relatively large. Taking comprehensive consideration, this distance was set at 62 mm in this study. After design and arrangement, the total number of rotary tillage blades was 66. In the middle ditching area, the blades at all 5 cross-sections were bent outward, and the specific arrangement was shown in Fig. 6.

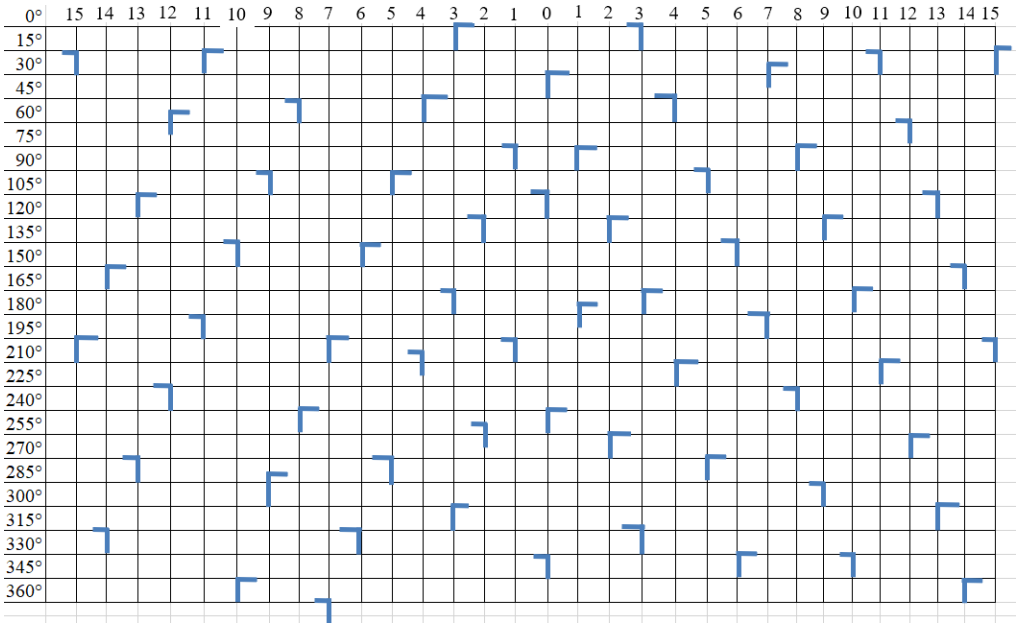

Fig. 6 - Rotary blade arrangement diagram

Design of ditching and ridging components

(1) Design of Ditch-Cleaning Shovel

For the middle ditching operation, the soil in the middle area needs to be thrown to both sides. As can be seen from the rotary tillage blade arrangement diagram in Fig. 6, four rotary tillage curved blades are arranged at the middle cross-section of the tiller, including 2 right-handed blades and 2 left-handed blades. The four rotary tillage blades at the two cross-sections on the left side of the middle cross-section are left-handed, while those at the two cross-sections on the right side are right-handed. The purpose is to throw the soil clods cut in the middle area axially to both sides.

Subsequently, the residual soil clods in the central zone are displaced laterally by the ditch-cleaning shovel, thus forming the middle ditch. The structure of the enveloping ditch-cleaning shovel is shown in Fig. 7. The ditch-cleaning shovel is connected to the rotary tiller frame via a pin shaft, allowing the shovel to rotate about the pin shaft. The inner curved surface of the ditch-cleaning shovel is attached to the rotary tiller shaft, with a clearance of *t*, maintained between them. The inner curved surface of the ditch-cleaning shovel is divided into four segments: the soil entry segment AB, the preparation segment BC, the transition segment CD, and the installation and fixing segment. At the start of operation the rotary tillage blades enter the preparation segment BC to get ready for soil cutting, and then move into the soil entry segment AB to begin cutting the soil. After cutting the soil, the blades rotate approximately half a revolution, lift the soil upward, and throw it backward through the housing. Segments AB and BC are the sections where the rotary tillage blades carry the soil. To enable the rotary tillage blades to actively scrape off the soil-straw mixture adhering to the ditch-cleaning shovel, segments AB and BC are designed as circular arcs with the same radius, which are concentric with the rotation center of the rotary tiller shaft and envelop the motion trajectory of the blade tips. The arc length of segment AB is determined by the ditch depth and the radius of the cutter roller. The longer the arc length of segment BC, the better the enveloping effect of the ditch-cleaning shovel, and the less the amount of soil and straw adhering and tangling to it. However, an excessively long arc length tends to cause the shovel handle to move forward, resulting in reduced structural strength (*Liao Yitao et al., 2020*).

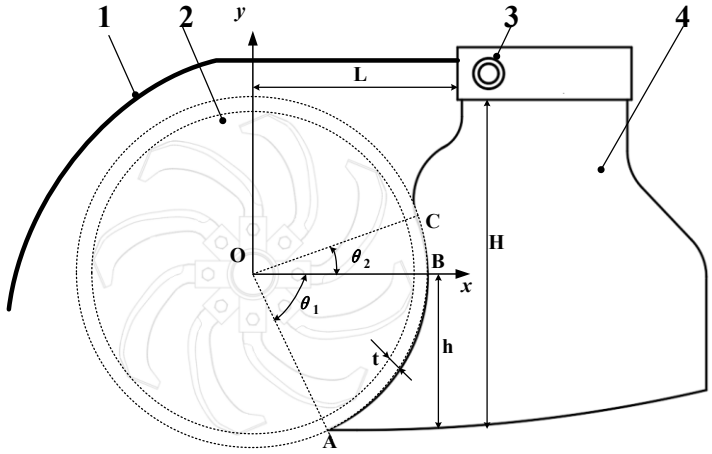

Fig. 7 - Curve of envelope ditch cleaning shovel

1. Housing; 2. Rotary tiller shaft; 3. Pin shaft; 4. Ditch-cleaning shovel;

Legend: point O is the rotation center of the rotary tiller shaft; curve AB represents the soil entry segment of the ditch-cleaning shovel; curve BC represents the preparation segment; curve CD represents the transition segment; r is the rotation radius of the rotary tillage blade; R is the radius of the enveloping curve of the ditch-cleaning shovel.θ_1 is the central angle of the curve of the soil entry segment; θ_2 is the central angle of the curve of the preparation segment; h is the vertical distance from the lowest point of the ditch-cleaning shovel to the rotation center of the rotary tiller shaft; H is the vertical distance from the lowest point of the ditch-cleaning shovel to the bottom surface of the fixed beam; L is the horizontal distance from the front side surface of the fixed beam to the rotation center

① Radius of the enveloping arc

Segments AB (soil entry section) and BC (preparation section) of the ditch-cleaning shovel are circular arcs concentric with the rotation center of the rotary tiller shaft, with the enveloping radius slightly larger than that of the cutter roller. The clearance *t* between the ditch-cleaning shovel and the cutter roller should be as small as possible (*Sineyakov, 1981*) while avoiding interference. According to the provisions of *GB/T 5669-2008 (National Technical Committee for Agricultural Machinery Standardization*, *2009*), the limit deviation value of the center distance of the fixing holes on the shovel handle is 2.0 mm. Combined with the results of preliminary tests, the value of *t* was determined to be 5 mm.

② Central angle of the arc of the soil entry segment

A coordinate system is established with the rotation center of the rotary tiller shaft as the origin, the horizontal direction as the -axis and the vertical direction as the -axis. The central angle corresponding to the arc of the soil entry segment AB is θ_1. According to the difference between the proposed ditching depth and rotary tillage depth, the distance h between point A of the ditch-cleaning shovel and the rotation center of the rotary tillage blade is determined. The value of *h* should be slightly smaller than the radius of the rotary tiller shaft *(Sineyakov, 1981*), and h=240 mm is adopted in this design. The value of θ_1=73.74° is obtained through geometric calculation.

③ Central angle of the arc of the preparation segment

Segment BC (preparation section) affects the throwing performance of the soil-straw mixture. An excessively small central angle θ_2 of the arc of the preparation section will cause some adherents to accumulate on the upper part, thereby leading to soil clogging of the machine; an excessively large θ_2 will result in an overly long movement stroke of the thrown soil along with the blades, increasing energy consumption and reducing the machine's trafficability (*Sineyakov, 1981*). Considering the installation position of the frame and the structural space comprehensively, the value of θ_2 is set at 26°.

④ Width of the Ditch-Cleaning Shovel

The width of the ditch-cleaning shovel determines the width of the final formed ditch. According to agronomic requirements, the width of the field ditch ranges from 15 to 20 cm. To meet the agronomic requirements of most regions, the ditch width should be selected as large as possible. In this study, the ditch width is set at 20 cm, and thus the width of the ditch-cleaning shovel is determined to be 20 cm.

(2) Design of the Flat Ridge Slitting Roller

After reverse rotary tillage, soil throwing and ditching operations, the soil structure achieves a layered effect, with the soil in the middle ditching section thrown to both sides of the ditch. Although the preliminary leveling of the ridge surface soil is realized through the optimized arrangement of rotary tillage blades, it still fails to meet the soil flatness requirements for transplanting. Soil compaction can squeeze the raised soil on the surface, improve soil flatness, enhance soil firmness and play a role in soil moisture conservation. The designed flat ridge slitting roller is shown in Fig. 8.

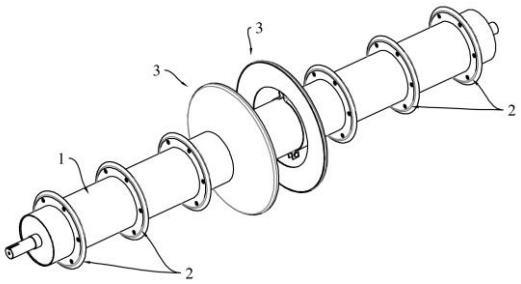

Fig. 8 - Diagram of soil flatting slitting roller

1.Soil leveling roller body; 2. Slitting disc; 3. Conical disc

As shown in Fig. 9, the minimum radius R of the soil leveling roller shall satisfy the requirement that:

$$R \geq \frac{b}{1-\cos\alpha} \tag{9}$$

where:

R is radius of the soil leveling roller, [mm]; b is rolling depth of the soil leveling roller, [mm]; α is turning angle of the soil leveling roller, [°].

For loose dryland soil, the required rolling depth *b* ranges from 10 to 30 mm. However, in rice stubble fields, due to the high soil moisture content, the rolling depth should not be excessively large. According to production practice, the rolling depth *b* is determined to be 6 to 20 mm, and a value of 6 mm is adopted in this study. To ensure the normal operation of the soil leveling roller, the condition $\alpha \leq 20°$ should be satisfied, and a value of 20° is selected herein. Substituting the above parameters into Formula (9), the calculation results shows that the radius of the soil leveling roller should meet $R \geq 100$mm. Since the soil leveling roller is a driving component, an excessively large radius will significantly increase power consumption. Therefore, the radius of the soil leveling roller is set at 100 mm in this design.

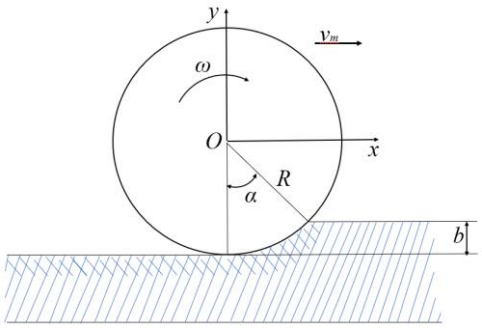

Fig. 9 - Working principle of soil flatting roller

The rotational speed of the soil leveling roller directly determines the flatness of the ridge surface. To avoid soil accumulation in front of the soil leveling roller, empirical data shows that the rotational speed of the soil leveling roller should be higher than the forward speed of the ridging machine. This can increase the compaction frequency of the soil on the ridge surface per unit area per unit time, thereby improving the flatness of the ridge surface. Therefore, within a certain range, the higher the rotational speed of the soil leveling roller, the better the flatness of the ridge surface. The forward speed v_m of the combined transplanter ranges from 0.8 to 1.2 m/s, and a value of 1.0 m/s is adopted in this design. The linear speed v of the soil leveling roller should satisfy the condition $v \geq 2v_m$.Combined with the radius of the soil leveling roller of 100 mm, the calculation shows that the rotational speed n_p of the soil leveling roller should meet $n_p \geq 191$ r/min.

After the soil leveling roller flattens the ridge surface, favorable conditions are provided for slitting. For structural compactness, the slitting disc is mounted together with the soil leveling roller and rotates synchronously with the roller to cut a transplanting slot, as shown in Fig. 8.

The width of the slitting disc is determined by the width of the seedling block. Given that the width of the seedling block is 20 mm, and considering soil rebound, the width of the slitting disc is set at 22 mm.

The diameter of the slitting disc is determined by the transplanting depth. The typical transplanting depth for rapeseed mat seedlings is 40 mm. Combined with the 100 mm radius of the soil leveling roller, the main body radius of the slitting disc is set at 140 mm. To achieve better slitting performance, the rim of the slitting disc is designed with an acute angle. Since the part cut by the acute angle falls outside the transplanting depth range of seedlings and the acute-angle area will be partially filled with soil after slitting, the overall radius of the slitting disc—including the acute-angle rim—is set at 155 mm.

The theoretical cross-section of the ditch formed by the ditch-cleaning shovel is rectangular. In practice, however, the side walls are uneven and prone to collapse. The conical disc serves to compact both sides of the ditch, resulting in a smooth trapezoidal cross-section. According to agronomic requirements, the ditch depth ranges from 18 to 20 cm, and a depth of 18 cm is adopted in this study. Combined with the 100 mm radius of the soil leveling roller, the radius of the conical disc is set at 280 mm. Considering the soil rebound on both sides of the ditch, the cone angle is determined to be 12°.

Field experiment and verification

The experiment was conducted in Baima Town, Nanjing City, Jiangsu Province, China, in November 2024. The soil of the experimental field was yellow loam. Prior to the experiment, the soil bulk density was measured by the soil sampling and weighing method, which showed that the soil bulk density was 1.32 g/cm³ in the 0–10 cm layer and 1.64 g/cm³ in the 10–20 cm layer. A soil moisture meter was used to determine the soil moisture content, with the values being 24.3% in the 0–5 cm layer, 28.7% in the 5–10 cm layer, 31.2% in the 10–15 cm layer, and 33.8% in the 15–20 cm layer. The experimental site is shown in Fig. 10. The main instruments used in the experiment included the SC-900 soil compaction meter, MS-350 soil moisture meter, electronic balance, electronic scale, and steel tape.

Fig. 10 - Test equipment and site

Experiment 1: Soil fragmentation test of the topsoil layer, this experiment was conducted to investigate the effects of the structural parameters of the grass barrier grid and soil retaining soft curtain on the soil layered structure. The key parameter of the grass barrier grid is the grid bar spacing, which is generally 60–80 mm; the spacing can be appropriately increased to avoid soil clogging. The front-rear distance between the soil retaining soft curtain and the rotary tiller shaft should be minimized on the premise of preventing soil accumulation. A full factorial experiment was carried out with the grass barrier grid spacing and soil retaining soft curtain distance as experimental factors, and the soil fragmentation rate of the topsoil layer as the evaluation index. The soil fragmentation rate of the topsoil layer was calculated using Formula (10), and the factor level table is presented in Table 1.

Experiment 2: Whole machine test. The experimental factors were selected under the conditions that the structural parameters such as the arrangement and layout of rotary tillage blades and ditch-cleaning shovels had been determined, and the parameters of grass barrier grid spacing and soil retaining soft curtain distance, which affect soil throwing performance, had been confirmed through experimental research. According to the motion analysis of rotary tillage blades, their motion trajectory is related to the rotational speed of the rotary tiller shaft and the forward speed of the machine. This is mainly because the tractor's output power take-off (PTO) is fixed; once the rotary tillage transmission ratio is determined, the rotational speed of the rotary tiller shaft is fixed and cannot be adjusted, while the operating speed is variable. Therefore, the forward speed of the machine exerts a significant influence on seedbed preparation. After rotary tillage, the ridge surface is leveled by the active soil leveling roller, and the compaction effect is related to the relative linear speed of the soil leveling roller in contact with the soil. Thus, the rotational speed of the soil leveling roller has an important impact on ridge surface flatness and exhibits an interaction effect with the forward speed of the machine. Therefore, this study selected three experimental factors, namely, the forward speed of the machine V_m, the rotational speed of the rotary tiller shaft n, and the rotational speed of the soil leveling roller n_p, with three levels set for each factor. The factors were coded as x_1, x_2 and x_3. The levels of each factor were determined based on theoretical analysis results and practical experience. The operating speed range of the unit was set at 0.8–1.4 m/s according to actual operating experience, the rotational speed range of the soil leveling roller was 180–240 r/min, and the rotational speed range of the rotary tiller shaft *n* was 250–350 r/min. In accordance with the requirements of *GB/T 5668-2008 (National Technical Committee for Agricultural Machinery Standardization, 2008)* and combined with the agronomic requirements for dryland transplanting of rapeseed mat seedlings, the experimental indicators were selected as soil fragmentation rate, straw incorporation rate, and ridge surface flatness, which were calculated using Formulas (11–13). The total length of the test plot was 30 m, with the middle 20 m designated as the stable measurement area. Each working condition was repeated 3 times, and the average value was taken as the final result. For the field test, a three-factor, three-level response surface test was designed using the Box-Behnken design in Design-Expert 8.0 software, and the factor coding is presented in Table 2.

(1) Determination Method for Soil Fragmentation Rate of the Topsoil Layer

The measurement points are consistent with those for the residual vegetation amount on the tilled soil surface, with an area of 0.5 m × 0.5 m per measurement point. Within the range of 8 cm below the soil surface, the soil fragmentation rate of the topsoil layer is defined as the percentage of the mass of soil clods with the maximum side length less than 2 cm to the total soil mass. The calculation formula is as follows:

$$S_t = m_1/m_2 \times 100\% \quad (10)$$

where: S_t is soil fragmentation rate of the topsoil layer, [%]; m_1 is mass of soil clods with the maximum side length less than 2 cm in the entire tillage layer at the measurement point, [kg]; m_2 is mass of soil within the range of 8 cm below the soil surface in the entire tillage layer over an area of 0.5 m × 0.5 m at the measurement point, [kg].

(2) Determination Method of Soil Fragmentation Rate

The measurement points are consistent with those for the residual vegetation amount on the tilled soil surface, with an area of 0.5 m × 0.5 m per measurement point. Within the range of 15 cm below the surface of the tillage layer, the soil fragmentation rate is defined as the percentage of the mass of soil clods with the maximum side length less than 4 cm relative to the total soil mass. The calculation formula is as follows:

$$Y_1 = \frac{m_a}{m_b} \times 100\% \quad (11)$$

where: Y_1 is soil fragmentation rate, [%]; m_a is mass of soil clods with the maximum side length less than 4 cm in the entire tillage layer at the measurement point, [kg]; m_b is mass of soil within the range of 15 cm below the surface of the entire tillage layer over an area of 0.5 m × 0.5 m at the measurement point, [kg].

(3) Straw Incorporation Rate

Randomly select one point within the measurement area of each travel pass, and measure the mass of all unburied straw within an area of 1 m × 1 m. The calculation formula for the straw incorporation rate is as follows:

$$Y_2 = \frac{M_q - M_h}{M_q} \times 100\% \quad (12)$$

where:

Y_2 is straw incorporation rate, [%]; M_q is straw mass per unit area before tillage, [g/m²]; M_h is unburied straw mass per unit area after tillage, [g/m²].

(4) Ridge Surface Flatness

Before the experiment, the reference height for soil flatness was measured, with the average surface height being 21 mm. Five measurement points were selected within the stable measurement area, and the working width was divided into 10 equal parts. The surface heights before and after the operation were measured respectively. The calculation formula for soil flatness is as follows:

$$Y_3 = \sqrt{\frac{\sum_{i=1}^{n_i}(a_{ji} - a_j)^2}{n_j}} \quad (13)$$

where:

Y_3 is soil flatness, [mm]; a_j is surface height of the j-th travel pass, [mm]; a_{ji} is surface height of the i-th point in the j-th travel pass, [mm]; n_i is number of the i-th measurement point; n_j is number of measurement points in the j-th travel pass.

Table 1

Factor levels for the surface soil fragmentation test in the tillage layer

Level	Factor	
	Grid Bar Spacing A [mm]	Soil Retaining Soft Curtain Distance B [mm]
1	65	400
2	70	450
3	75	500
4	80	550

Table 2

Factor levels for the device performance test

Level	Forward Speed x_1 [m/s]	Rotary tiller shaft speed x_2 [r/min]	Leveling roller speed x_3 [r/min]
-1	0.8	250	180
0	1.1	300	210
1	1.4	350	240

RESULTS

Surface soil fragmentation test in the tillage layer

A full-factorial experiment was conducted using grid bar spacing and soil-retaining soft curtain distance as the experimental factors, with the soil fragmentation rate of the surface soil in the tillage layer as the evaluation index. A total of 16 experimental groups were set up (Table 3)

Table 3

Scheme and results of soil fragmentation test on the surface of tillage layer

No.	Grid Bar Spacing A [mm]	Soil Retaining Soft Curtain Distance B [mm]	Soil fragmentation rate of tillage layer [%]
1	65	400	83.64
2	65	450	85.65
3	65	500	89.25
4	65	550	88.61
5	70	400	89.99
6	70	450	92.06
7	70	500	93.12
8	70	550	88.27

No.	Grid Bar Spacing A [mm]	Soil Retaining Soft Curtain Distance B [mm]	Soil fragmentation rate of tillage layer [%]
9	75	400	91.62
10	75	450	94.03
11	75	500	98.02
12	75	550	86.86
13	80	400	87.12
14	80	450	86.56
15	80	500	92.25
16	80	550	85.36
k_1	86.79	88.09	
k_2	90.86	89.58	
k_3	92.63	93.16	
k_4	87.82	87.28	
R	23.38	20.27	

Table 4

Variance analysis of soil fragmentation test on the surface of cultivated layer

Data Source	Sum of Squares	Degrees of Freedom	Mean Square	F-value	P-value
Model	168.65	6	28.11	5.46	0.01
Grid Bar Spacing A/mm	87.32	3	29.11	5.65	0.02
Soil Retaining Soft Curtain Distance B/mm	81.32	3	27.11	5.26	0.02
Residual	46.36	9	5.15		
Total	215.00	15			

Note: P<0.01, extremely significant; 0.01≤P<0.05, significant.

According to Tables 3 and 4, the *P*-values (< 0.05) indicate that both factors in the model have a significant effect on the soil fragmentation rate, with the grid bar spacing exerting a more significant influence than the soil retaining soft curtain distance. Based on the *k*-values, the optimal grid bar spacing is determined to be 75 mm, and the optimal soil retaining soft curtain distance is 500 mm.

Complete machine test

A total of 17 groups of experiments were conducted according to the *Box-Behnken design*, and the experimental scheme is shown in Table 5. In the table x_1, x_2 and x_3 represent the coded values of the factors including machine forward speed, rotary shaft speed and leveling roller speed, respectively.

Table 5

Device test scheme and results

No.	Machine Forward Speed x_1 [m/s]	Rotary Shaft Speed x_2 [r/min]	Leveling Roller Speed x_3 [r/min]	Soil fragmentation rate Y_1 [%]	Straw Incorporation Rate Y_2 [%]	Ridge Surface Flatness Y_3 [mm]
1	0	-1	1	87.98	86.57	19.11
2	0	0	0	84.83	82.23	18.61
3	0	-1	-1	93.17	80.31	16.71
4	1	0	-1	86.32	82.78	18.69
5	0	0	0	85.34	81.68	18.73
6	-1	0	-1	96.52	86.89	15.14
7	0	0	0	84.82	79.24	18.33
8	1	-1	0	85.99	82.53	20.38
9	0	0	0	88.79	80.67	18.16
10	0	1	-1	93.71	76.91	16.38
11	1	1	0	76.82	74.34	19.92
12	-1	0	1	89.91	88.65	17.15
13	0	1	1	82.29	79.76	18.42
14	-1	1	0	90.97	74.83	16.18
15	1	0	1	78.23	92.21	21.35
16	-1	-1	0	94.84	82.78	16.98
17	0	0	0	83.65	77.89	19.26

Quadratic regression analysis and multiple regression fitting were performed on the experimental results using Design-Expert 8.0 software, and the regression equations of three experimental indicators, namely soil fragmentation rate Y_1, straw incorporation rate Y_2 and ridge surface flatness Y_3, were obtained.

$$\begin{cases} Y_1 = 86.23 - 5.61x_1 - 2.27x_2 - 3.91x_3 + 2.29{x_3}^2 \\ Y_2 = 80.34 - 0.1613x_1 - 3.29x_2 + 2.54x_3 + 1.92x_1x_3 + 2.51{x_1}^2 - 4.23{x_2}^2 + 4.78{x_3}^2 \\ Y_3 = 18.62 + 1.86x_1 - 0.285X_2 + 1.14x_3 + 0.0872{x_1}^2 - 0.3403{x_2}^2 - 0.6227{x_3}^2 \end{cases} \quad (14)$$

Analysis of variance (ANOVA) and significance test of regression coefficients were carried out for the quadratic regression model, and the ANOVA results of the experimental indicators are shown in Table 6.

Table 6

Variance analysis

Source of Variation	*p*-Value Y_1	*p*-Value Y_2	*p*-Value Y_3
model	0.0008	0.0008	< 0.0001
x_1	< 0.0001	0.7821	< 0.0001
x_2	0.0099	0.0006	0.0462
x_3	0.0005	0.0027	< 0.0001
x_1x_2	0.192	0.9418	0.6257
x_1x_3	0.6988	0.0463	0.362
x_2x_3	0.1334	0.3183	0.6059
${x_1}^2$	0.9456	0.0141	0.6078
${x_2}^2$	0.1157	0.0009	0.0745
${x_3}^2$	0.0438	0.0005	0.0064
Lack of Fit	0.5823	0.6915	0.9485

Note: P<0.01, extremely significant;0.01≤P<0.05, significant.

According to Table 6, all the experimental models were significant (P＜0.05). The analysis of variance for the soil fragmentation rate showed that the primary factor, machine forward speed x_1, had the most significant effect on the indicator. The order of the influence degree of each factor on the indicator was $x_1 > x_3 > x_2$. The analysis of variance results for straw incorporation rate indicated that the primary factors, rotary shaft speed x_2 and leveling roller speed x_3, had relatively significant effects on the indicator, and the influence priority of each factor on the indicator was $x_2 > x_3 > x_1$. The analysis of variance results for ridge surface flatness indicated that the primary factors, machine forward speed x_1 and leveling roller speed x_3 had relatively significant effects on the indicator, and the influence priority of each factor on the indicator was $x_3 > x_1 > x_2$.

To obtain the optimal motion parameters of the seedbed preparation device for the rapeseed mat seedling transplanter, the optimization module of Design-Expert 13.0 software was adopted. With the maximization of soil fragmentation rate, straw incorporation rate and ridge surface flatness as the optimization objectives, the regression model in Equation (14) was optimized and solved. The optimal results showed that when the machine forward speed was 0.8 m/s, the rotary shaft speed was 243 r/min, and the leveling roller speed was 180 r/min, the soil fragmentation rate reached 98.92%, the straw incorporation rate was 87.81%, and the ridge surface flatness was 15.14mm.

Overall machine verification test

To verify the optimization results, field verification tests were conducted on the obtained optimal parameter combination under the same operating conditions as previously described. The tests were repeated three times, and the average values were adopted. The results are shown in Table 7.

Table 7

Verification test results

Item	Soil fragmentation rate [%]		Straw Incorporation Rate [%]		Ridge Surface Flatness [mm]	
	Test	Average Value	Test	Average Value	Test	Average Value
Result	95.83		91.86		16.54	
	97.31	96.66	90.73	90.69	15.33	15.61
	96.84		89.48		14.97	

The test results showed that under the optimal operating parameters obtained by software calculation, the average soil fragmentation rate after operation was 97.72%, the average straw incorporation rate was 89.68%, and the average ridge surface flatness was 15.61 mm.

The errors relative to the software-predicted values were 2.28%, 3.28% and 3.1%, respectively. These results indicated that the accuracy of the regression models for soil fragmentation rate, straw incorporation rate and ridge surface flatness could meet the requirements of the machine's operating performance.

CONCLUSIONS

To address the problems of large straw biomass and heavy sticky soil in rice stubble fields, where traditional tillage methods struggle to crush soil, stubble and straw, fail to create a seedbed condition with a flat and fine surface, and lead to difficulties in transplanting rapeseed mat seedlings and low seedling establishment rate, this chapter proposes a seedbed preparation method combining reverse-rotation soil fragmentation and stubble burying with ridge leveling and slit cutting, and establishes a mathematical model for seedbed quality. The device reduces soil compaction and improves seedbed uniformity, offering a practical solution for no-till transplanting in rice stubble fields. The main research work is as follows:

(1) The theoretical analysis yielded the arrangement mode of reverse rotary tillage blades, and the kinematic analysis determined the rotational speed of the rotary tiller shaft to be 310 r/min. Through the theoretical analysis of soil-throwing performance and experimental research on key parameters, the optimal spacing of the grass barrier grid was obtained as 75 mm, and the optimal distance of the soil-retaining soft curtain was 500 mm. The structural parameters of the furrow cleaning shovel were confirmed by theoretical analysis, which also revealed that the radius of the soil leveling roller should be 100 mm with a rotational speed of ≥ 191 r/min, the radius of the conical disc should be 280 mm, and the pressure of the elastic preloading mechanism should range from 4104 N to 6840 N. Ultimately, the overall structure of the seedbed preparation device was finalized.

(2) In the field experiment, three factors, namely the machine forward speed, rotary tiller roller speed and soil leveling roller speed, were selected, while the soil fragmentation rate, straw incorporation rate and seedbed surface flatness were taken as the evaluation indicators for seedbed quality. A three-factor, three-level response surface experiment was carried out. Mathematical regression models for the three seedbed quality indicators were established based on the experimental data, and an optimization analysis was conducted on these regression models. The optimal results were obtained as follows: when the machine forward speed was 0.8 m/s, the rotary tiller roller speed was 243 $r \cdot min^{-1}$ and the soil leveling roller speed was 180 $r \cdot min^{-1}$, the soil fragmentation rate reached 98.92%, the straw incorporation rate was 87.81%, and the surface flatness was 15.14 mm. Experimental verification was performed on the optimized results, and the errors between the experimental results and the software-predicted values were 2.28%, 3.28% and 3.1%, respectively.

ACKNOWLEDGEMENT

This research was supported by the national key R & D project, 2023YFD2001001; the China Postdoctoral Science Foundation, 2023M740866; the research and development and promotion project of new equipment and new technology of agricultural machinery in Jiangsu Province, NJ2024-01; China Agriculture Research System of MOF and MARA, CARS-12.

REFERENCES

[1] Alagbo O.O., Saile M., Spaeth M., Schumacher M., Gerhards R., (2024). Development and testing of a precision hoeing system for re-compacted ridge tillage in maize, *Heliyon*, vol10, no.23, Amsterdam/Netherlands. DOI:10.1016/j.heliyon.2024.e40527

[2] Chetan F., Pop A.I., Chetan C., Gaga I., Simon A., Urdă C., Popa A., Călugăr R.E., Rusu T., Moraru P.I. , (2025). Impact of tillage system and mineral fertilization on weed suppression and yield of winter wheat, *Agronomy*, vol.15, no.8, pp.1904, Basel/Switzerland.DOI:10.3390/agronomy15081904

[3] Dai F., Han Z., Zhang K. Hu J., Feng Y., Zhang F., (2011). Development present situation of straw returned combined machine used in China (我国机械化秸秆还田联合作业机的现状与发展),*Chinese Agricultural Mechanization*, no.6, pp.42-45,37, Nanjing/China. DOI: https://doi.org/10.3969/j.issn.1006-7205.2011.06.010

[4] Durr C., Aubertot J.N., (2000). Emergence of seedlings of sugar beet (Beta vulgaris L.) as affected by the size, roughness and position of aggregates in the seedbed. *Plant and Soil*, vol.219, pp.211-220, Netherlands. DOI: https://doi.org/10.1023/A:1004723901989

[5] Ding W., Wang Y., Peng S., (2001). Comparison experiment and property analysis of up-cut and down-cut rotary blades (正、反转旋耕刀性能分析及切土扭矩比较试验), *Journal of Nanjing Agricultural University*, vol.24, no.01, pp.113-117, Nanjing/China.

[6] Ding W., Wang Y., Peng S., (2003). Comparison on performances of up-cut and down-cut rotary tillage(正、反转旋耕不同耕作性能的比较), *Journal of Nanjing Agricultural University*, vol.26, no.03, pp.106-109, Nanjing/China.

[7] Ferreira C.J.B., Tormena C.A., Severiano E.C., Nunes M.R., Menezes C.C.E., Antille D.L., Preto V.R.O., (2023), Effectiveness of narrow tine and double-discs openers to overcome shallow compaction and improve soybean yield in long-term no-tillage soil, *Soil & Tillage Research*, vol.227, pp.105622, Amsterdam/Netherlands.DOI:10.1016/j.still.2022.105622

[8] Hakansson I., Myrbeck Å., Etana A., (2002). A review of research on seedbed preparation for small grains in Sweden, *Soil and Tillage Research*, vol.64, no.1-2, pp.23–40, Netherlands. DOI: https://doi.org/10.1016/S0167-1987（01）00255-0

[9] Jensen T., Karstoft H., Green O., Munkholm L.J., (2017). Assessing the effect of the seedbed cultivator leveling tines on soil surface properties using laser range scanners, *Soil and Tillage Research*, vol.167, pp.54–60, Netherlands. DOI: https://doi.org/10.1016/j.still.2016.11.006

[10] Jia H., Chen Z., Guo H., Li R., Li X., (2000). Study on working principle of rotary tillage and stubble cutting and design of universal knife roller (旋耕碎茬工作机理研究和通用刀辊的设计), *Transactions of the Chinese Society for Agricultural Machinery*, vol.31, no.04, pp.29-32, Beijing/China. DOI: https://doi.org/10.3969/j.issn.1000-1298.2000.04.008

[11] Luo J., (2019). *Design and experimental study of wheat uniform seeder (小麦匀播播种机设计及试验研究)*, MSc Thesis, Jiangsu University. Zhenjiang/China.

[12] Liao Q., Bu X., Sun W., Wei G., Zhang Q., Wang P., (2020). Development of driven plow-rotary combined tillage machine for construction of rational tillage in rape seedbeds (构建油菜种床合理耕层的驱动型犁旋联合耕整机研究), *Transactions of the Chinese Society for Agricultural Machinery*, vol.51, no.11, pp.74-84, Beijing/China. DOI: https://doi.org/10.6041/j.issn.1000-1298.2020.11.008

[13] Li Z., Xu K., Yan S., Xu L., Yang Y., Wang Z., (2020). Structural design and test of stubble cutter roller for two-axis rotary stubble mitigation machine (双轴式旋耕灭茬机灭茬刀辊结构设计与试验), *Journal of Agricultural Mechanization Research,* vol.42, no.04, pp.117-124,131, Heilongjiang/China. DOI: https://doi.org/10.3969/j.issn.1003-188X.2020.04.024

[14] Liao Y., Gao L., Liao Q., Zhang Q., Liu L., Fu Y., (2020). Design and test of side deep fertilizing device of combined precision rapeseed seeder (油菜精量联合直播机深施肥装置设计与试验), *Transactions of the Chinese Society for Agricultural Machinery*, vol.51, no.2, pp.65-75, Beijing/China. DOI: https://doi.org/10.6041/j.issn.1000-1298.2020.02.008

[15] Nidal H.A., Randall C.R., (2003). A nonlinear 3D finite element analysis of the soil forces acting on a disk plow, *Soil and Tillage Research*, vol.74, no.2, pp.115–124, Netherlands. DOI: https://doi.org/10.1016/S0167-1987（03）00152-1

[16] National Technical Committee for Agricultural Machinery Standardization of China., (2009). *Rotary Tiller GB/T 5668-2008*, Standards Press of China: 17, Beijing/China.

[17] Peng B., (2014). *Modeling and simulation of soil cutting dynamics of rotary of mini-tiller*(微耕机刀辊切土动力学建模及仿真), MSc Thesis ,Master Dissertation of Southwest University, Chongqing/China.

[18] Riegler N.P., Moitzi G., Prankl J., Huber J., Karner J., Wagentristl H., Vincze M., (2020). Machine vision for soil roughness measurement and control of tillage machines during seedbed preparation, *Soil and Tillage Research*, vol.196, pp.104351, Netherlands. DOI: https://doi.org/10.1016/j.still.2019.104351

[19] Shibusawa S., (1993). Reverse-rotational rotary tiller for reduced power requirement in deep tillage. *Journal of Terramechanics*, vol.30, no.3, pp.205-217, England. DOI: https://doi.org/10.1016/0022-4898（93）90007-K

[20] Siniacov., Panno., Li Q.G., (1981). *Theory and Calculation of Soil Tillage Machinery (土壤耕作机械的理论和计算)*, China Agricultural Machinery Press, Beijing/China.

[21] Ucgul M., Fielke J.M., Saunders C., (2014). 3D DEM tillage simulation: Validation of a hysteretic spring

(plastic) contact model for a sweep tool operating in a cohesionless soil, *Soil and Tillage Research*, vol.144, pp.220–227, Netherlands. DOI: https://doi.org/10.1016/j.still.2013.10.003

[22] Zhang C., Xia J., Zhang J., Zhou H., Zhu Y., Wang J., (2019). Design and experiment of knife roller for six-head spiral straw returning cultivator (六头螺旋秸秆还田耕整机刀辊设计与试验), *Transactions of the Chinese Society for Agricultural Machinery*, vol.50, no.03, pp.25-34, Beijing/China. DOI:https://doi.org/10.6041/j.issn.1000-1298.2019.03.003

[23] *** Chinese Academy of Agricultural Mechanization Sciences., (2007). *Agricultural Machinery Design Manual (农业机械设计手册)*, China Agricultural Science and Technology Press, ISBN 978-7-80233 335-2, Beijing/China.